The 2016 World Congress on
Advances in Civil, Environmental, and Materials Research (ACEM16)
Jeju Island, Korea, August 28-September 1, 2016

The Impact of Curing Regime, Silica Fume Fineness, and Fiber Lenghts on UHPFRC's

Hasan Şahan AREL[1], Merve ÖNER[2]

[1]*Faculty of Architecture, İzmir University, Gürsel Aksel Bulvarı, No:14, 35350, Üçkuyular / İzmir / Turkey, corresponding author*
[2]*Interior Architecture and Environmental Design, İzmir University, Gürsel Aksel Bulvarı, No:14, 35350, Üçkuyular / İzmir / Turkey*

Abstract

The effects of silica fume fineness and fiber aspect ratio on the compressive strength and impact resistance of ultra-high-performance fiber-reinforced concrete (UHPFRC) were experimentally investigated. To this end, UHPFRC mixtures were manufactured by combining silica fumes with different finenesses (specific surface areas: 17,200, 20,000, and 27,600 m²/kg) and hooked-end steel fibers with various aspect ratios (lengths: 8, 13, and 16 mm). Samples were subjected to standard curing, steam curing, and hot-water curing. Compressive strength tests were conducted after 7-, 28-, 56-, and 90-day curing periods and an impact resistance experiment was performed after the 90th day. The steam-cured mixture of silica fumes presenting a specific surface area of 27,600 m²/kg and 16 mm-long fibers demonstrated the best mechanical properties. Moreover, the impact resistance increased with increasing fiber aspect ratio.

1. INTRODUCTION

Characterized by compressive and tensile strengths exceeding 150 and 8 MPa, respectively (Habel K. and Gauvreau, 2008), ultra-high-performance fiber-reinforced concrete (UHPFRC) results from the combination of various fibers and high-performance concrete (HPC) with a low water–cement (w/c) ratio (Allena and Newston 2010; Xiao et al. 2014) It displays significantly higher toughness, durability, and strength comparison with its conventional analog (Yu et al., 2014; Lampropoulos et al. 2016; Farnam et al., 2010). It also exhibits high compressive strengths using pozzolans, such as silica fume and granulated blast furnace slag (Máca et al., 2014; Corinaldesi and Moriconi, 2012; Jungwirth and Muttoni, 2004; Habel et al., 2006; Aldahdooh et al., 2013). In addition, its mechanical properties depend on the type, amount, and length of the fiber (Hannawi et al., 2015; Park et al., 2012; Yoo et al., 2014). Yoo et al. (2014) investigated the effects of fiber lengths on the compressive strength of UHPFRC by producing samples using 13, 16.3, 19.5, and 30 mm-long fibers at a rate of 2%. Samples prepared with 16.3 and 19.5 mm-long fibers presented the highest (204 MPa) and lowest compressive strengths (94 MPa), respectively. Yang et al. (2009) studied the effects of curing methods on the mechanical properties of UHPFRC by mixing the concrete with steel fibers for a water–binder ratio of 0.15 using 657 kg/m³ cement, 429.8 kg/m³ granulated blast-furnace slag (GGBS), 119.4 kg/m³ silica fume, and 1050 kg/m³ aggregate sand. Silica sand, fine ordinary sand type I, fine ordinary sand type II,

and recycled glass cullet acted as fine aggregates, and the mixtures were cured at water temperatures of 20 and 90 °C for 7, 14, 28, 56, and 91 days. After 28 days at 90° C, UHPFRC samples comprising fine ordinary sand type I aggregates exhibited the highest compressive strength (179 MPa), whereas specimens comprising recycled glass cullent displayed the lowest value (165 MPa). At 90 °C, samples comprising fine ordinary sand type II achieved the best flexural strength (25 MPa). Nehdi et al. (2015) evaluated the compressive and splitting tensile strengths of tunnel lining materials obtained using UHPFRC comprising fibers of various lengths and compositions. Specifically, steel fibers measuring 8, 12, and 16 mm were added at ratios of 1%, 3%, and 6%. Specimens containing 12 mm-long fibers exhibited the highest compressive strength (173 MPa) at a ratio of 2% but the lowest splitting tensile strength (39 MPa) at a ratio of 6%. Aoude et al. (2015) compared the tensile and compressive strengths of UHPFRC comprising 657 kg/m³ cement, 418 kg/m³ GGBS, 119 kg/m³ silica fume, 1051 kg/m³ silica sand, 40 kg/m³ superplasticizer, 185 kg/m³ water, and 2% steel fibers. After a 28-day curing period, respective compressive and tensile strengths of 150.56 and 9.07 MPa, were noted, while the elastic modulus reached 45.55 GPa.

2. RESEARCH SIGNIFICANCE

Numerous independent studies have examined the effect of fiber length, curing method, and mixture ratios on the mechanical properties of UHPFRC (Yu et al., 2014; Corinaldesi and Moriconi, 2012; Tayeh et al., 2013; Kim et al., 2011). The current study assessed the impact of silica fume finenesses, fiber aspect ratios, and curing methods on the mechanical properties of UHPFRC. Also, it determined the influence of silica fume fineness on the workability of fresh concrete and setting time. The obtained results were compared with previous independently obtained findings.

3. EXPERİMENTAL STUDY

3.1. Materials

3.1.1. Cement

Portland cement (CEM I type 42.5 R) presenting properties in agreement with the TS EN 197-1 Standard (2012) was used as binder. Cement has a specific gravity 3.1 g/cm³ and specific surface area 415 m²/kg.

3.1.2. Silica Fume

Three different types of silica fumes (SF1–SF3) displaying properties in agreement with the TS EN 13263-1+A1 Standard (2011) were purchased from Eti Antalya Electrometallurgy Inc. Their specific surface areas were determined by the Brunauer–Emmett–Teller nitrogen adsorption method after grinding. Specific surface areas: SF1: 17,200, SF2: 20,000, and SF3: 27,600 m²/kg.

3.1.3. Quartz Sand

Quartz sand displaying properties in agreement with the TS EN 12904 Standard (2010) was obtained from Antalya, Turkey. Quartz sand has a specific gravity 2.8 g/cm³, specific surface area 255 m²/kg and 45 µm sieve residue 42.05%.

3.1.4. Steel Fiber

Hooked-end steel fibers measuring 8, 13, and 16 mm in length and 0.2 mm in diameter were chosen in accordance with the TS EN 10513 Standard (2013).

3.1.5. Chemical Additives

HE 200 hyper plasticizers were used as additives in agreement with the TS EN 934-2+A1 Standard (2011).

3.3. Concrete Mixture Preparation and Production

The UHPFRC mixtures were prepared in accordance with the TS EN 206 Standard (2014). Three different types of silica fume with fineness values of 16400 m²/kg (SF1), 20000 m²/kg (SF2), and 27600 m²/kg (SF3) were used in the mixtures. In the mixtures produced with a 0.19 water/cement ratio, steel fibers with lengths of 8 mm, 13 mm, and 16 mm were used. The prepared mixtures were poured into specific molds to form cubes (150 mm × 150 mm × 150 mm) and cylinders (100 × 200 mm) for compressive strength, and impact resistance tests, respectively. All mixtures were defined as a type of silica fume fineness–length of fiber-mixture number. That is, SF1-8 mm corresponds to a SF1-type silica fume, and 8 mm length steel fiber. Material amounts in the UHPFRC mixtures are shown in Table 1 along with mixture codes.

Table 1. Material amounts and mixture ratios (kg/m³)

Specimens	Components (kg/m³)										
	Cement	Quartz	Water	SF 1	SF 2	SF 3	L_f 8 mm	L_f 13 mm	L_f 16 mm	SP	w/c
SF1-8 mm	640	1170	135	214	-	-	145	-	-	35	0.21
SF1-13 mm	640	1170	135	214	-	-	-	145	-	35	0.21
SF1-16 mm	640	1170	135	214	-	-	-	-	145	35	0.21
SF2-8 mm	640	1170	135	-	214	-	145	-	-	37.5	0.21
SF2-13 mm	640	1170	135	-	214	-	-	145	-	37.5	0.21
SF2-16 mm	640	1170	135	-	214	-	-	-	145	37.5	0.21
SF3-8 mm	640	1170	135	-	-	214	145	-	-	40	0.21
SF3-13 mm	640	1170	135	-	-	214	-	145	-	40	0.21
SF3-16 mm	640	1170	135	-	-	214	-	-	145	40	0.21

SF: silica fume, SP: superplasticizer, w/c: water/cement ratio, L_f: length of steel fiber.

3.4. Sample Curing

Samples were cast and subjected to standard curing, steam curing, and hot water curing for 7, 28, 56, and 90 days. Samples were removed from their molds 24 h after casting and allowed to stand in tap water pools at 20±2 °C in accordance with the TS EN 12390-2 Standard (2010) for standard curing. The maximum temperature was set to 65 °C and applied for 10 h of steam curing. The temperature was initially kept at 20 °C for 4 h before being raised to 65 °C at a rate of 0.18 °C/min. Next, this temperature was maintained 16 h. At the beginning of the 20th h, the temperature was decreased to 20 °C at a rate of 0.18 °C /min and kept constant. Steam curing was performed in accordance with the ASTM C 684-99 Standard (1999), and sample setting times were determined before the curing process. Once set, steam cured samples were stored at 22 °C in 90% humidity until mechanical testing. Samples were removed from the molds 24 h after the casting and allowed to stand in curing pools set at 80 °C for hot water curing. Samples left in the pool for 3 days were stored at 22 °C in 90% humidity until mechanical testing was performed.

4. EXPERIMENTAL RESULTS

The consistency and the setting time determination tests were conducted in fresh concrete mixtures. After casting, compressive strength, and impact resistance tests were conducted for the cured samples.

4.1. Fresh Concrete Experiments

4.1.1. Determination of the Setting Time

Setting times were determined according to the TS 2987 Standard (2011). Figure 1 shows the setting times of UHPFRC mixtures prepared with SF1–3.

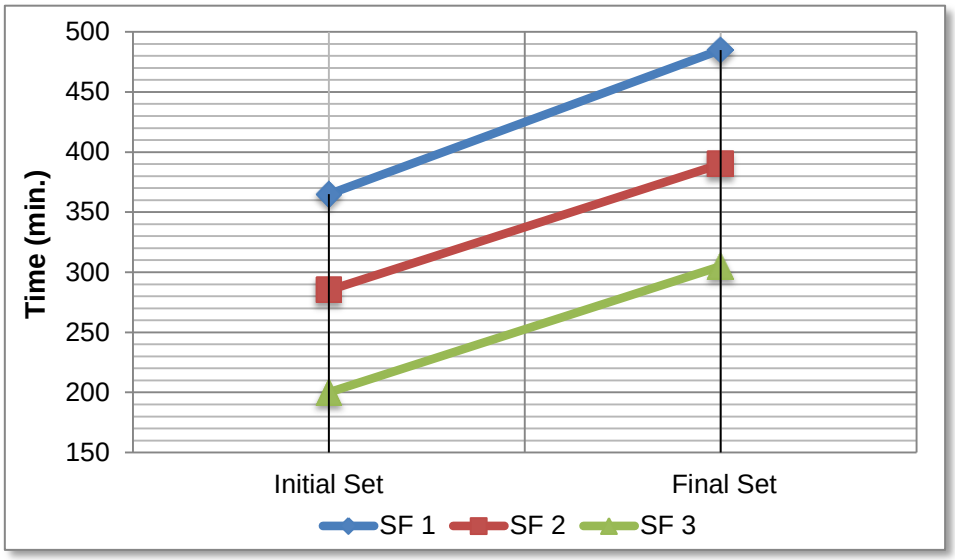

Figure 1. Changes in setting times for UHPFRC mixtures containing different silica fumes

Setting times decreased with increasing silica fume fineness. The initial setting times were determined as 365, 285, and 200 min for mixtures containing SF1, SF2, and SF3,

respectively, which represents an 80–85 min decrease with increasing silica fume fineness. Final setting times of 485, 390, and 305 min were obtained for mixtures containing SF1, SF2, and SF3, respectively, which corresponds to an 85–95 min reduction with increasing silica fume fineness. Zhang and Islam (2012) found that 2% nanosilica-containing concrete mixtures required 90 and 100 min shorter initial and final setting times, respectively, than their 2% silica fume-containing equivalents. These nanosilica materials presented BET surface areas of 200.1 m²/g.

4.1.2. Consistency Determination

The consistency of UHPFRC mixtures was evaluated according to the TS EN 12350-5 Standard (2001), and the resulting flow values are shown in Figure 2.

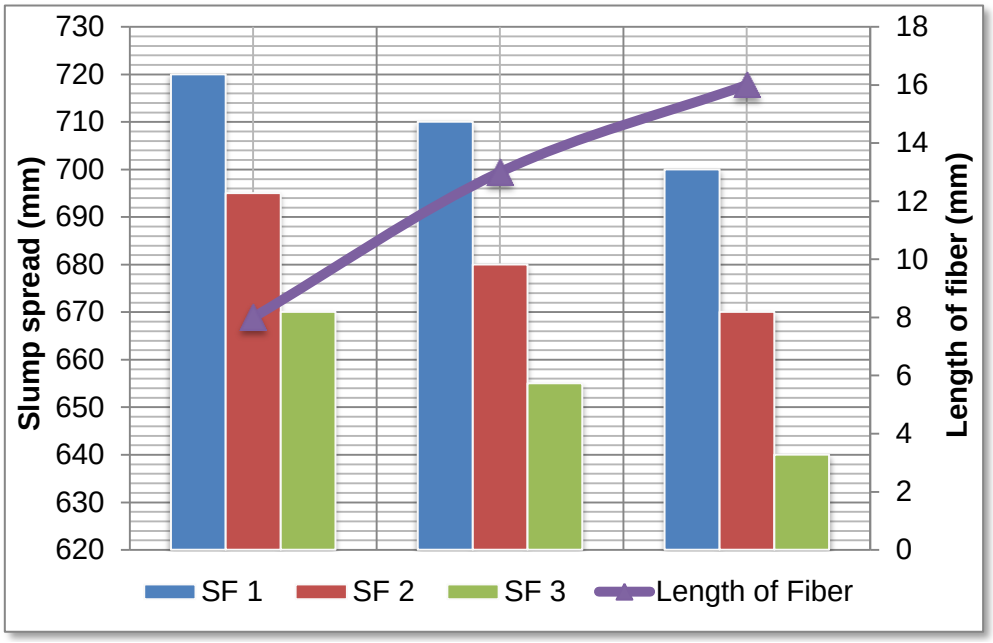

Figure 2. Flow spread values of the UHPFRC mixtures

Flow spread values decreased with increasing silica fume fineness and fiber length (Fig. 2). Flow spread values of 720, 695, and 670 mm were obtained for SF1, SF2, and SF3-based mixtures comprising 8 mm-long fibers, respectively. For 13 mm-long fibers, these values amounted to 695, 680, and 670 mm, respectively. This decrease may stem from the increase in viscosity and adhesion with increasing silica fume fineness. These results were consistent with previous findings. Specifically, Nehdi et al. (2015) discovered that flow spread values decreased with increasing fiber length. Flow spread values of 800, 790, and 780 mm were observed for fiber lengths of 8, 12, and 16 mm, respectively. Similarly, Mobini et al. (2015) found that flow spread values decreased with the increasing nanosilica fineness for HPFRC mixtures. Furthermore, the flow spread value decreased with increasing fiber content because of the increase in mixture viscosity.

4.2. Compressive Strength Testing

Compressive strengths were assessed using cured cubic samples (dimensions: 150 mm × 150 mm × 150 mm) according to the TS 12390-3 Standard (2010). Each data point corresponded to the average of six independent tests performed on the 28th, 56th, and 90th curing day.

4.2.1. Compressive Strengths of Samples Subjected to Standard Curing

The compressive strengths of UHPFRC samples subjected to standard curing are shown in Figure 3. The changes observed on the 28th and 90th day as a function fiber length are shown in Figure 4.

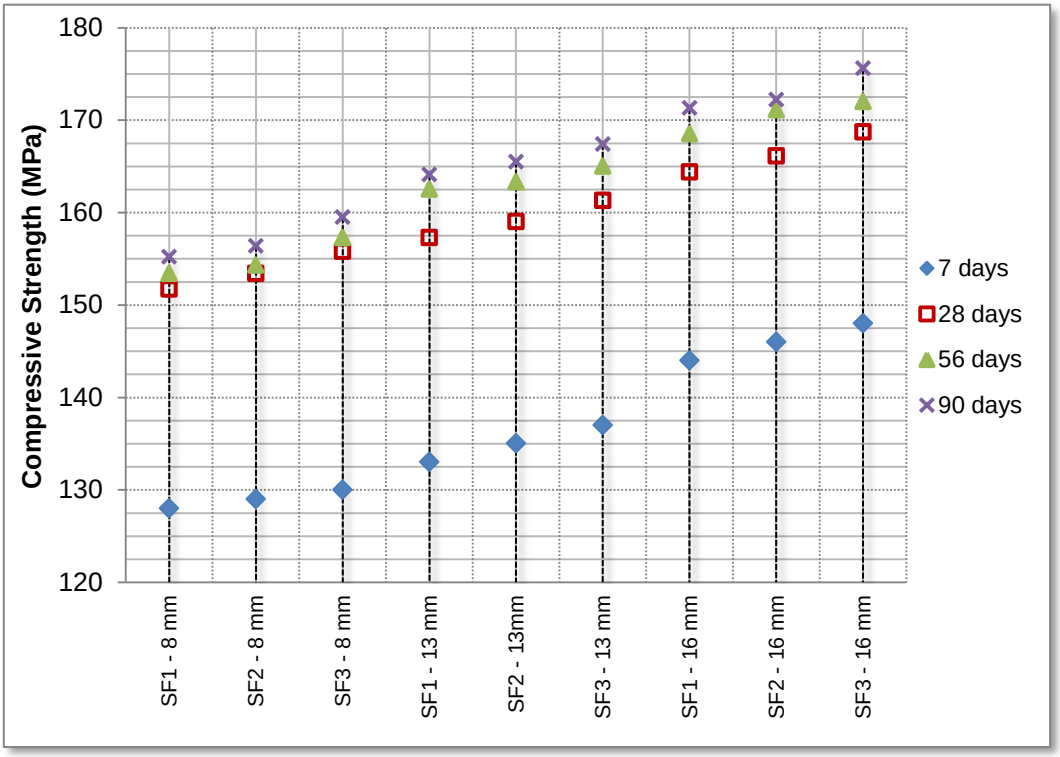

Figure 3. Compressive strength of samples subjected to standard curing after 7, 28, 56, and 90 days

The compressive strength increased with increasing silica fume fineness and fiber length. This trend was considerably more pronounced for silica fume fineness than for fiber length. This may stem from two phenomena. First, calcium hydroxide ($Ca(OH)_2$) derived from the hydration of calcium silicates (C_2S ve C_3S), the main constituent of cement, interacted with silica fume and filled voids present in the aggregate cement paste with extra calcium silicate hydrate (C-S-H) gels. Second, the silica fume particles became stickier, enhancing physical adherence at the aggregate–cement interface. The highest compressive strength (175.6 MPa) was observed for sample SF3-16 mm. In contrast, sample SF1-8 mm achieved the lowest compressive strength (151.7 MPa). This suggested that silica fume reacted with water-dissolved ($Ca(OH)_2$) and generated voids in concrete, thereby increasing the compressive strength of the material by

creating extra C-S-H gels. Compressive strengths obtained for samples SF2-8 mm and SF3-8 mm surpassed the values for sample SF1-8 mm by 3.7% and 8.3%, respectively, after 28 d. These strengths exceeded the respective values for sample SF1-8 mm by 5.9% and 9.8% after 56 days and by 5.7% and 10.3% after 90 days. For the same curing period, samples gained 2.8% and 10.3% in compressive strength with increasing silica fume fineness. The compressive strength rose by 1% and 2.1% with increasing fiber length. Jaturapitakkul et al. (2004) studied the effect of silica fumes presenting different finenesses on high-strength concrete using HPC samples comprising SF1 with a median particle size (d50) of 89.00 µm and a silica fume substitute with a d50 value of 105 µm. After 28 d, the compressive strength for the SF1 silica fume substitute, which was finer, amounted to 92, while that for the SF2 silica fume substitute amounted to 87 MPa, which was 5.7% lower than that for the SF1 silica fume substitute. After 56 d, the compressive strengths equaled 97 and 89 MPa for the SF1 substitute and SF2, respectively. Moreover, consistent with the current results, they increased with increasing silica fume fineness. Habel et al. (2006) obtained a compressive strength of 175 MPa for a UHPFRC mixture comprising 1050 kg/m³ cement, 730 kg/m³ quartz sand, 275 kg/m³ silica fume, 470 kg/m³ steel fiber, 190 kg/m³ water, and 35 kg/m³ superplasticizer at a w/c ratio of 0.18 after 28 days of curing. Also, the compressive strength increased more slowly after 90 days than during the first 28 d. A lower amount of cement was used here compared to a previous study (Habel et al., 2006). However, a similar compressive strength was achieved by increasing the silica fume fineness, revealing the essential role of this material feature on compressive strength.

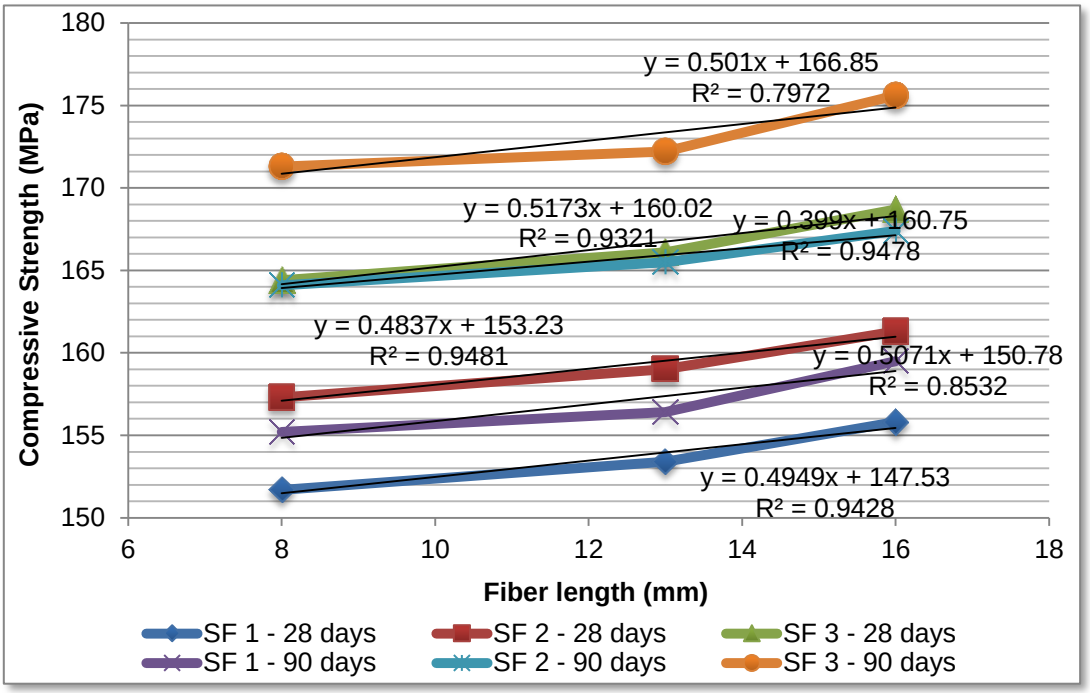

Figure 4. 28th and 90th day compressive strength–fiber length relationship of the samples subjected to standard curing

The compressive strength increased with increasing fiber length (Figure 4), leading to optimal values for 16 mm-long steel fiber regardless of silica fume fineness. This

increase reached a maximum of 2.1% when the fiber ratio increased. Similarly, Yoo et al. (2014) investigated the effect of steel fibers of different lengths on the mechanical properties of UHPFRC. After 28 d, the compressive strength amounted to 190 and 193 MPa for 13 and 16.3 mm-long steel fibers, respectively, which represents a 1.5% increase.

4.2.2. Compressive Strengths of Steam-Cured Samples

The compressive strengths of steam-cured samples are shown in Figure 5.

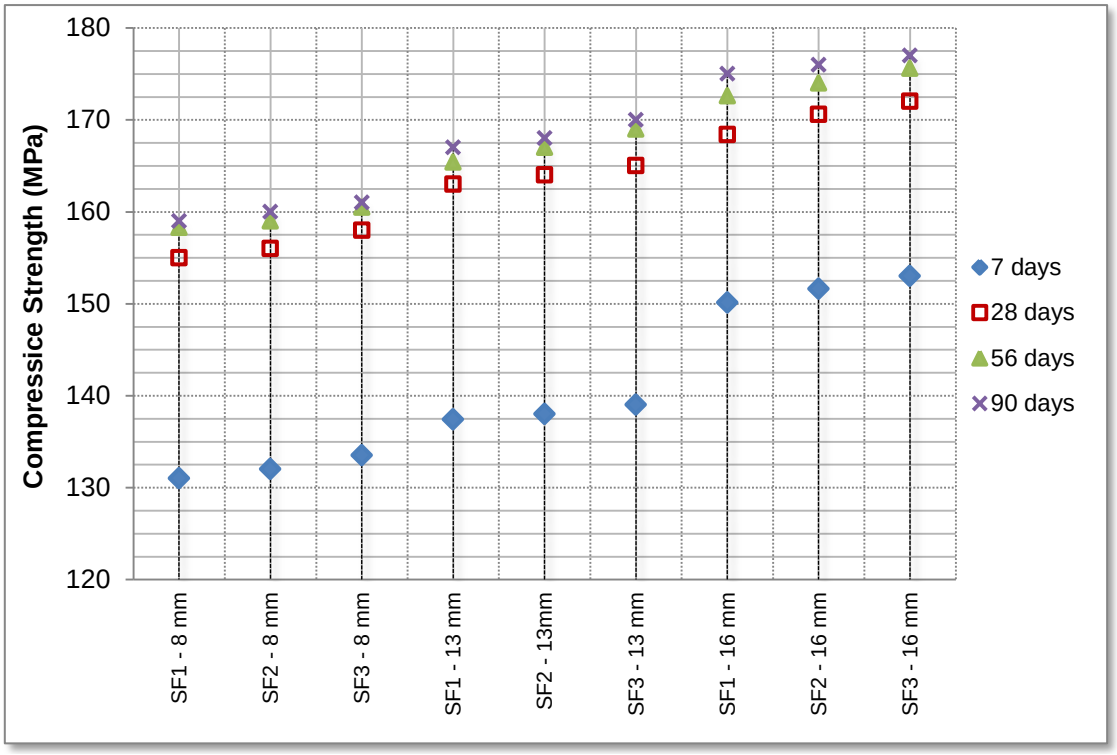

Figure 5. Compressive strengths of steam-cured samples after 7, 28, 56, and 90 days

The increase in compressive strength slowed down after 28 days of steam curing (Figure 5). Concrete samples gained 86% of their ultimate strength during the first week. This may result from the hydration of the abundant C_3S in the cement, creating C-S-H gels. However, the gain in strength decelerated afterward. Sample SF3-16 mm presented a compressive strength of 153 and 172 MPa after 7 and 28 d, respectively, which corresponds to a 12.4% increase. However, a value of 175.6 MPa was obtained after 56 d, which represents a 2% increase. After 90 d, the rate of increase was approximately 0.8%. This phenomenon may be attributed to the change of C-S-H composition due to temperature fluctuations, which as a hydration product, displayed fast hydration during the first week. Moreover, the compressive strength increased with increasing silica fume fineness. This may result from the reaction between silica fume and (Ca(OH)2), which caused capillary breaks in the concrete upon dissolution in water, produced C-S-H, and increased physical adherence that filled the voids at the cement–

aggregate interface. The highest compressive strength (176 MPa) was observed for sample SF3-16 mm after 90 days while the lowest value (131 MPa) was obtained for sample SF1-8 mm after 28 days. Geseoğlu et al. (2015) measured the compressive strengths of UHPFRC samples after 28, 90, 180, and 360 days. These values were 129 and 133 MPa after 28 days under standard and steam curing conditions, respectively, and reached 133 and 140 MPa after 90 days of standard and steam curing before slowly decreasing beyond 180 d.

4.2.3. Compressive Strengths of Hot Water-Cured Samples

The compressive strengths of hot water-cured samples are shown in Figure 6.

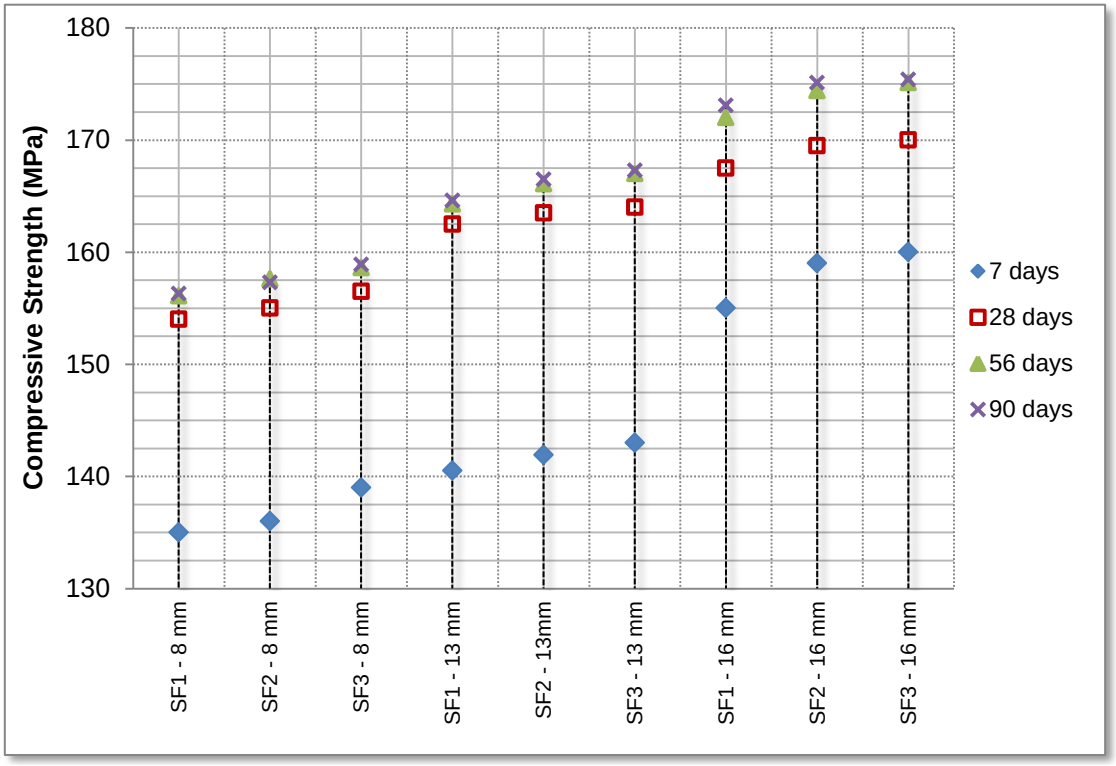

Figure 6. 7th, 28th, 56th and 90th day compressive strength results for samples subjected to hot water curing

The initial increase in compressive strength was more pronounced during hot water curing than in steam and standard equivalents (Figure 6). Similar to steam curing, this may originate from the C-S-H composition, which as a hydration product, changes according to temperature and displays faster hydration during the first week. Moreover, the compressive strength of concrete increased with increasing silica fume fineness, which was consistent with other curing conditions (Figure 6). Sample SF3-16 mm displayed the highest compressive strength (175.4 MPa) after 90 days while sample SF1-8 mm achieved the lowest value (135 MPa) after 7 d. For a constant fiber length, SF3 samples exhibited 3% and 6.2% gains in compressive strength between 7 and 56

days. This gain only amounted to 0.1% beyond 56 days. This may stem from the fast C_2S ve C_3S hydrations, the binding of the resulting calcium hydroxide ($Ca(OH)_2$), and the subsequent C-S-H gel formation. Similarly, Yang et al. (2009) studied the effects of water curing at 20 and 90 °C on the mechanical properties of UHPFRC mixtures containing different types of sand. Samples cured in 90 °C water displayed 20% greater compressive strength than their counterparts cured at 20 °C. However, the compressive strength remained constant after 56 days.

4.4. Impact Resistance Tests

Impact resistance tests were performed using cylindrical samples (dimensions: 100 × 200 mm) in accordance with the ACI Committee 544 recommendation (1996). Specifically, a 4.54 kg steel hammer was allowed to drop repeatedly onto the center of the sample from a height of 300 mm. When the experiment was implying, it was taken the advantage of the methods implied in similar studies in literature (Song et al., 2005; Nili and Afroughsabet, 2010; Marar et al., 2001). These tests were conducted after a 90-d curing period so that silica fume effects started to even out, facilitating comparisons with previous studies. The impact energy *E* was calculated using the following formulae:

$$H = gt^2/2 \quad (1)$$

$$V = gt \quad (2)$$

$$E = 1/2\ mV^2N \quad (3)$$

and m = W/g, where *V* is the velocity of the hammer at impact, *g* is the gravitational acceleration, *m* is the mass of the hammer, *H* is the height of the fall, *N* is the number of blows, W is the weight of the hammer, and *t* is the time required by the hammer to fall from height *H*. The impact resistance test results of samples subjected to standard, steam, and hot water curing are shown in Figures 7, 8, and 9, respectively.

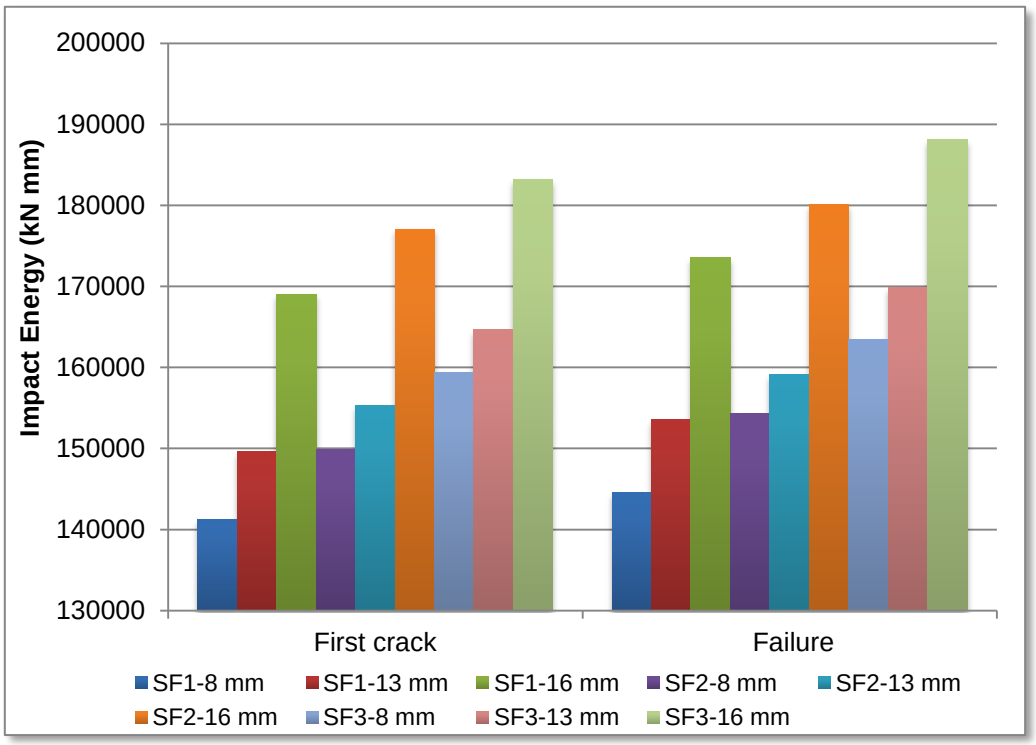

Figure 7. Impact resistance test results for samples after 90 days of standard curing

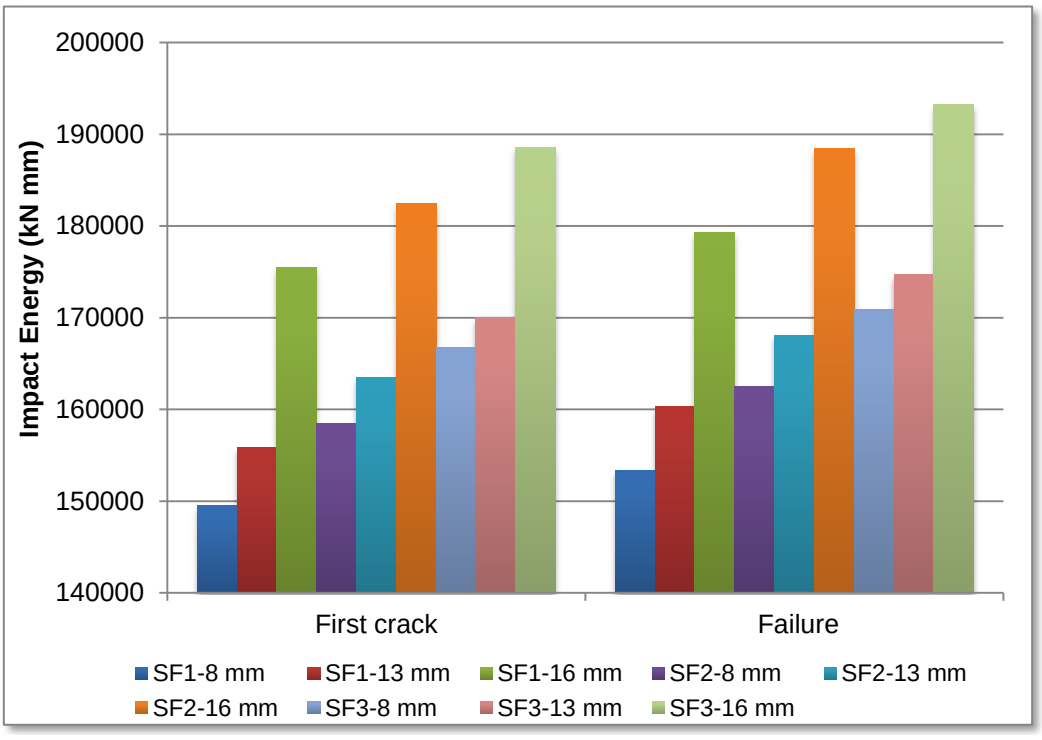

Figure 8. Impact resistance test results of samples after 90 days of steam curing

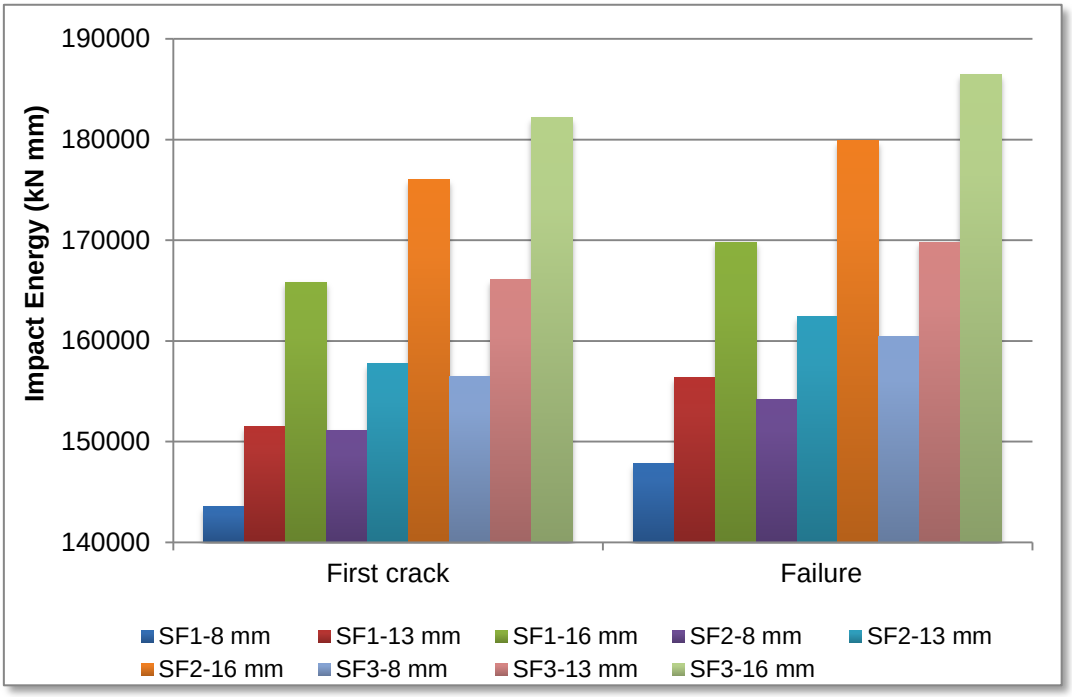

Figure 9. Impact resistance test results of samples after 90 days of hot water curing

The impact resistance increased with increasing silica fume fineness and fiber aspect ratio for all curing conditions (Figures 7–9), leading to a maximum for sample SF3-16 mm. This may stem from three phenomena. First, the reaction between the main constituents of cement (C_2S and C_3S) and water-produced crystals, which created C-S-H gels that provided additional binding by reacting with silica fume. Second, silica fume increased the physical adherence at the cement–aggregate interface. Third, concrete toughness increased with increasing fiber aspect ratio because fibers prevented microcracks from expanding and progressing upon impact. Several studies have previously demonstrated that fiber length strongly affected the impact resistance of concrete. Mohammedi et al. (2009) evaluated the effects of aspect ratio on the impact resistance of SFRC samples comprising 50 and 25 mm-long fibers. Impact failure energies averaged 723.5 and 378.1 kN mm for samples incorporating 50 and 25 mm-long fibers, respectively. Nili and Afroughsabet (2010) investigated the effects of polypropylene fibers on the impact resistance and mechanical properties of concrete. The impact resistance increased by 30% with increasing compressive strength after 90 days for samples with silica fume containing steel fibers. This may stem from the contribution of silica fume to the pozzolanic property and crack resistance of fibers. The impact resistance reached a maximum of 8117.7 kN mm for a polypropylene fiber-containing sample presenting a compressive strength of 73.26 MPa and a w/c ratio of 0.36. Gupta et al. (2015) determined the factors affecting the impact resistance of rubber-fiber-containing concrete samples produced without as well as with 5% and 10% silica fume replacement at various w/c ratios. The impact number for the first crack increased with increasing silica fume replacement ratio and rubber fiber content. At a w/c ratio of 0.35, samples produced with 5% rubber fiber and 10% silica fume

replacement showed an impact number of 100 for the first crack. This impact number was 300 for samples involving 25% rubber fiber and 10% silica fume replacement.

5. CONCLUSION

Under the effect of standard curing, samples produced with SF1 silica fume displayed results between 4% and 5.7% lower and 10% lower in comparison with those displayed by samples produced with SF2 and SF3 silica fumes, respectively.

Under all curing conditions, the compressive strength increased between 1.5% and 2.1% with increasing fiber content.

The best compressive strength value was observed in the SF3-16 mm sample when subjected to steam curing after 90 days (177 MPa); and the worst compressive strength value was observed in the SF1-8 mm sample when subjected to standard curing after 7 days (128 MPa).

The impact resistance was directly proportional to the compressive strength value, and the SD-16 mm sample subjected to steam curing displayed the maximum value (193241 kN).

After 56 days, the samples subjected to standard curing, steam curing, and hot water curing continued to gain 2%, 0.8%, and 0.22% compressive strength, respectively. With steam and hot water curing, the compressive-strength increase rate decreased after 56 days. However, in the next ages, a separate study is required to investigate the compressive strength values.

The best compressive strength and impact resistance results were obtained from the SF3 silica fume, whose specific surface area was 27600 m²/kg.

Acknowledgement

This paper was published in “Results in Physics”, 2016, http://dx.doi.org/10.1016/j.rinp.2016.09.016. However, this paper was completely rearranged, reinterpreted and rewritten for *"The 2016 World Congress on Advances in Civil, Environmental, and Materials Research (ACEM16)"*

REFERENCES

ACI Committee 544. ACI 544.2R-89: Measurement of properties of fiber reinforced concrete. ACI Manual of Concrete Practice 1996; Part 5: Masonry, Precast Concrete and Special Processes, American Concrete Institute

Aldahdooh, M.A.A., N.M. Bunnori, Johari M.A.M., (2013). “Evaluation of ultra-high-performance-fiber reinforced concrete binder content using the response surface method” *Materials & Design*, Vol. **52**, 957–965 doi:10.1016/j.matdes.2013.06.034

Aoude, H., Dagenais, F.P., Burrell, R.P., Saatcioglu M., (2015). “"Behavior of ultra-high performance fiber reinforced concrete columns under blast loading” *International Journal of Impact Engineering*, Vol. **80**, 185–202. doi:10.1016/j.ijimpeng.2015.02.006

ASTM C 684-99, Standard Test Method for Making, Accelerated Curing, and Testing Concrete Compression Test Specimens, *Annual Book of ASTM Standards, 1999*

Corinaldesi, V. and Moriconi, G., (2012). "Mechanical and thermal evaluation of Ultra-High Performance Fiber Reinforced Concretes for engineering applications." *Construction and Building Materials*, Vol. **26**(1), 289–294. doi:10.1016/j.conbuildmat.2011.06.023

Farnam, Y., Mohammadi, S., Shekarchi, M., (2010). "Experimental and numerical investigations of low velocity impact behavior of high-performance fiber-reinforced cement based composite" *International Journal of Impact Engineering,* Vol. **37**(2), 220–229 doi:10.1016/j.ijimpeng.2009.08.006

Gesoğlu, M., Güneyisi, E., Nahhab, A.H., Yazıcı, H., (2015). "Properties of ultra-high performance fiber reinforced cementitious composites made with gypsum-contaminated aggregates and cured at normal and elevated temperatures" *Construction and Building Materials,* Vol. **93**, 427–438. doi:10.1016/j.conbuildmat.2015.05.130

Gupta, T., Sharma, R.K., Chaudhary S., (2015). "Impact resistance of concrete containing waste rubber fiber and silica fume." *International Journal of Impact Engineering,* Vol. **83**, 76–87. doi:10.1016/j.ijimpeng.2015.05.002

Habel, K. and Gauvreau, P. (2008). "Response of ultra-high performance fiber reinforced concrete (UHPFRC) to impact and static loading." *Cement and Concrete Composites,* Vol. **30** (10): 938–46. doi:10.1016/j.cemconcomp.2008.09.001

Habel, K., Viviani, M., Denarié, E., Brühwiler E., (2006). "Development of the mechanical properties of an Ultra-High Performance Fiber Reinforced Concrete (UHPFRC)." *Cement and Concrete Research*, Vol. **36**(7), 1362–1370. doi:10.1016/j.cemconres.2006.03.009

Hannawi, K., Bian, H., Prince-Agbodjan, W., Raghavan B., (2015). "Effect of different types of fibers on the microstructure and the mechanical behavior of Ultra-High Performance Fiber-Reinforced Concretes." *Composites Part B: Engineering*, Vol. **86**, 214–220. doi:10.1016/j.compositesb.2015.09.059

Jaturapitakkul, C., Kiattikomol, K., Sata, V., Leekeeratikul T., (2004) "Use of ground coarse fly ash as a replacement of condensed silica fume in producing high-strength concrete." *Cement and Concrete Research,* Vol. **34**(4), 549–55. doi:10.1016/S0008-8846(03)00150-9

Jungwirth J., Muttoni, A., (2004). "Structural behavior of tension members in Ultra High Performance Concrete." In: *International symposium on ultra high performance concrete*, Kassel, 553–46.

Kim, D.J., Park, S.H., Ryu, G.S., Koh, K.T., (2011). "Comparative flexural behavior of Hybrid Ultra High Performance Fiber Reinforced Concrete with different macro fibers" *Construction and Building Materials*, Vol. **25**(11), 4144–4155 doi:10.1016/j.conbuildmat.2011.04.051

Lampropoulos, A.P., Paschalis, S.A., Tsioulou, O.T., Dritsos, S.E., (2016). "Strengthening of reinforced concrete beams using ultra high performance fibre reinforced concrete (UHPFRC)." *Engineering Structures*, Vol. **106** 370–384. http://dx.doi.org/10.1016/j.engstruct.2015.10.042

Máca, P., Sovják, R., Konvalinka, P., (2014). "Mix design of UHPFRC and its response to projectile impact" *International Journal of Impact Engineering*, Vol. **63**, 158–163. doi:10.1016/j.ijimpeng.2013.08.003

Marar, K., Eren, Ö., Celik, T., (2001). "Relationship between impact energy and compression toughness energy of high-strength fiber-reinforced concrete." *Materials Letters,* Vol. **47**(4-5): 297–304. doi:10.1016/S0167-577X(00)00253-6
Mobini, M.H., Khaloo, A., Hosseini, P., Esrafili A., (2015). "Mechanical properties of fiber-reinforced high-performance concrete incorporating pyrogenic nanosilica with different surface areas." *Construction and Building Materials,* Vol. **101**(1), 130–140. doi:10.1016/j.conbuildmat.2015.10.032
Nehdi, M.L., Abbas, S., Soliman, A.M., (2015). "Exploratory study of ultra-high performance fiber reinforced concrete tunnel lining segments with varying steel fiber lengths and dosages" *Engineering Structures,* Vol. **101**, 733–742. doi:10.1016/j.engstruct.2015.07.012
Nili, M. and Afroughsabet, V., (2010). "Combined effect of silica fume and steel fibers on the impact resistance and mechanical properties of concrete." *International Journal of Impact Engineering,* Vol. **37**(8), 879–886. doi:10.1016/j.ijimpeng.2010.03.004
Park, S.H., Kima, D.J., Ryu, G.S., Koh, K.T., (2012). "Tensile behavior of Ultra High Performance Hybrid Fiber Reinforced Concrete." *Cement and Concrete Composites*, Vol. **34**(2), 172–184 doi:10.1016/j.cemconcomp.2011.09.009
Song, P.S., Wu, J.C, Hwang, S., Sheu, B.C., (2005). "Statistical analysis of impact strength and strength reliability of steel–polypropylene hybrid fiber-reinforced concrete." *Construction and Building Materials*, Vol. **19**(1), 1–9. doi:10.1016/j.conbuildmat.2004.05.002
Tayeh, B.A., Abu Bakar, B.H., Johari, M.A.M., Voo Y.L., (2013). "Evaluation of Bond Strength between Normal Concrete Substrate and Ultra High Performance Fiber Concrete as a Repair Material." *Procedia Engineering,* Vol. **54**, 554–563. doi:10.1016/j.proeng.2013.03.050
TS 2987 (2011). Determination of the concrete setting time by measurement of penetration resistance
TS EN 12350-5 (2001). Testing frehs concrete- Part 5: Flow table test
TS EN 12390-2 (2010). Testing hardened concrete - Part 2: Making and curing specimens for strength tests" Ankara, Turkey
TS EN 12904 (2010). Products used for treatment of water intended for human consumption - Silica sand and silica gravel
TS EN 13263-1+A1 (2011). Silica fume for concrete - Part 1: Definitions, requirements and conformity criteria
TS EN 197-1 (2012). Cement - Part 1: Composition, specification and conformity criteria for common cements
TS EN 206 (2014). Concrete - Property, performance, manufacturing and compliance with standards
TS EN 934-2 (2011). Admixtures for concrete, mortar and grout - Part 2: Concrete admixtures; Definitions, requirements, conformity, marking and labeling
TS EN ISO 10513 (2013). Prevailing torque type all-metal hexagon high nuts with metric fine pitch thread - Property classes 8, 10 and 12
Y. Mohammadi, R., Carkon-Azad, S.P., Singh, S.K., Kaushik., (2009). "Impact resistance of steel fibrous concrete containing fibers of mixed aspect ratio." *Construction and Building Materials,* Vol. **23**(1), 183–189. doi:10.1016/j.conbuildmat.2008.01.002

Xiao, J., Li, Z., Li, J. (2014). Shear transfer across a crack in high-strength concrete after elevated temperatures. *Construction and Building Materials*. Vol. **71**, 472–483 doi:10.1016/j.conbuildmat.2014.08.074

Yang, S.L., Millard, S.G., Soutsos, M.N., Barnett, S.J., Le, T.T. (2009). "Influence of aggregate and curing regime on the mechanical properties of ultra-high performance fiber reinforced concrete (UHPFRC)" *Construction and Building Materials,* Vol. **23**(6), 2291–2298 doi:10.1016/j.conbuildmat.2008.11.012

Yoo, D.Y., Kang, S.T., Yoon, Y.S., (2014). "Effect of fiber length and placement method on flexural behavior, tension-softening curve, and fiber distribution characteristics of UHPFRC" *Construction and Building Materials,* Vol. **64**, 67–81 doi:10.1016/j.conbuildmat.2014.04.007

Allena, S., Newtson, C.M. (2010). Ultra-high strength concrete mixtures using local materials. national ready mixed concrete association. *Concrete Sustainability Conference.* National Ready Mixed Concrete Association.

Yu R., Spiesz P., Brouwers, H.J.H. (2014). "Mix design and properties assessment of Ultra-High Performance Fibre Reinforced Concrete (UHPFRC)." *Cement and Concrete Research,* Vol. **56**, 29–39. doi:10.1016/j.cemconres.2013.11.002

Zhang, M.H. and Islam J., (2012). "Use Of Nano-Silica To Reduce Setting Time and Increase Early Strength of Concretes with High Volumes Of Fly Ash Or Slag." *Construction and Building Materials,* Vol. **29**, 573–580. doi:10.1016/j.conbuildmat.2011.11.013